Gastroenterology Report, 2022, 1–7

https://doi.org/10.1093/gastro/goac033
Original Article

ORIGINAL ARTICLE

Multi-frequency magnetic resonance elastography of the pancreas: measurement reproducibility and variance among healthy volunteers

Si-Ya Shi†, Liqin Wang†, Zhenpeng Peng†, Yangdi Wang, Zhi Lin, Xuefang Hu, Jiaxin Yuan, Li Huang, Shi-Ting Feng and Yanji Luo*

Department of Radiology, The First Affiliated Hospital, Sun Yat-sen University, Guangzhou, Guangdong, P. R. China

†These authors contributed equally to this article.
*Corresponding author. Department of Radiology, The First Affiliated Hospital, Sun Yat-sen University, No. 58, Second Zhongshan Road, Yuexiu District, Guangzhou, Guangdong 510080, China. Tel: +86-20-87755766-8471; Fax: +86-20-87615805; Email: luoyj26@mail.sysu.edu.cn

Abstract

Background Patients with chronic pancreatitis often have irreversible pancreatic insufficiency before a clinical diagnosis. Pancreatic cancer is a fatal malignant tumor in the advanced stages. Patients having high risk of pancreatic diseases must be screened early to obtain better outcomes using new imaging modalities. Therefore, this study aimed to investigate the reproducibility of tomoelastography measurements for assessing pancreatic stiffness and fluidity and the variance among healthy volunteers.

Methods Forty-seven healthy volunteers were prospectively enrolled and underwent two tomoelastography examinations at a mean interval of 7 days. Two radiologists blindly and independently measured the pancreatic stiffness and fluidity at the first examination to determine the reproducibility between readers. One radiologist measured the adjacent pancreatic slice at the first examination to determine the reproducibility among slices and measured the pancreas at the second examination to determine short-term repeatability. The stiffness and fluidity of the pancreatic head, body, and tail were compared to determine anatomical differences. The pancreatic stiffness and fluidity were compared based on sex, age, and body mass index (BMI).

Results Bland–Altman analyses (all $P > 0.05$) and intraclass correlation coefficients (all >0.9) indicated near perfect reproducibility among readers, slices, and examinations at short intervals. Neither stiffness ($P = 0.477$) nor fluidity ($P = 0.368$) differed among the pancreatic anatomical regions. The mean pancreatic stiffness was 1.45 ± 0.09 m/s; the mean pancreatic fluidity was 0.83 ± 0.06 rad. Stiffness and fluidity did not differ by sex, age, or BMI.

Conclusion Tomoelastography is a promising and reproducible tool for assessing pancreatic stiffness and fluidity in healthy volunteers.

Key words: tomoelastography; pancreas; healthy volunteers; stiffness; fluidity

Submitted: 8 December 2021; **Revised:** 8 April 2022; **Accepted:** 5 July 2022

Introduction

Pancreatic cancer is a highly fatal malignant tumor with a very low 5-year survival rate (<10%) because 80%–85% of cases are either unresectable or metastatic [1]. To achieve better patient outcomes, patients at high risk must be screened to detect pancreatic tumors during the early stages of the disease [2]. Similarly, patients with chronic pancreatitis (CP) can benefit from early detection because they often have irreversible pancreatic insufficiency before their clinical diagnosis, and active intervention can slow the disease's progression [3, 4]. Various imaging modalities for pancreatic diseases exist, but each has limitations [3]. An accurate diagnosis of pancreatic cancer or CP during the early stages remains challenging with the current imaging approaches.

New imaging techniques for pancreatic diseases have been presented based on the mechanical properties of the pancreas [5, 6]. Fibroblast activation and intratumoral collagen deposition gradually lead to dense fibrosis in pancreatic cancer [7]. CP is an inflammatory disease that causes progressive, irreversible fibrosis in the pancreas [8]. This fibrosis leads to increased pancreatic stiffness, which distinguishes it from the healthy pancreatic parenchyma [7–9]. Moreover, pancreatic cancer and autoimmune pancreatitis both exhibit increased fluidity [5]. Therefore, rather than focusing on morphological changes, clinicians should determine the mechanical properties of the pancreas to detect pancreatic diseases during the early stages.

Magnetic resonance elastography (MRE) facilitates the quantitative and spatially resolved determination of soft tissue viscoelastic parameters [10]. However, conventional elastography exhibits limited anatomical resolution owing to noise and insufficient elastic deformation, and thus currently cannot be used as a tomographic modality alone [10]. Tomoelastography is a novel MRE technique that includes compressed-air-driven surface-based actuators, multi-frequency wave data acquisition, and noise-robust data processing [10]. This technique provides quantitative maps of biomechanical properties that reveal highly resolved anatomic details [6, 11]. Until now, only a few studies have been conducted in which tomoelastography was used to characterize the viscoelastic properties of pancreatic tissues in patients [5, 6]. However, the reproducibility of using tomoelastography still requires further investigation because previous studies lacked the short-term and slices repeatability. Therefore, the present study was conducted to investigate the measurement reproducibility of tomoelastography for assessing pancreatic stiffness and fluidity of the pancreas and the variance among healthy volunteers as a function of anatomical region, sex, age, and body mass index (BMI).

Materials and methods

Healthy volunteer population

The Institutional Review Board of The First Affiliated Hospital, Sun Yat-sen University (Guangzhou, China) approved this prospective study (ethical approval reference number: 2021–721), which was conducted in accordance with the Declaration of Helsinki (as revised in 2013). All volunteers provided written informed consent. The inclusion criteria were healthy people with willingness to fast and undergo an MR examination and provision of signed informed consent. The exclusion criteria were as follows: age ≤18 years; BMI ≤16 or ≥28 kg/m^2; history of pancreatitis, pancreatic tumors, or pancreatic surgeries; history of diabetes or hypertension; history of malignancies; and claustrophobia. Forty-seven volunteers were enrolled. All volunteers underwent two examinations at intervals of 7 ± 2 days to test the feasibility and repeatability of the pancreatic tomoelastography.

Imaging acquisition

MR sequences

The MR examinations were performed using a 3.0-Tesla imaging system (MAGNETOM Prisma; Siemens Healthcare, Erlangen, Germany) with 18-channel phased-array surface coils. All volunteers were required to fast for 6–8 hours before the examination. The volunteers were placed in the supine position inside the imaging system, and all of them underwent the same scan protocol, which included coronal half-Fourier acquisition single-shot turbo spin-echo breath-hold T2-weighted imaging (T2WI), axial trigger turbo spin-echo fat-saturated (fs) T2WI, axial multi-echo Dixon volume-interpolated breath-hold (VIBE), and pancreatic tomoelastography. Table 1 lists the sequence parameters. Except for tomoelastography, all sequences were designed to check for pancreatic lesions.

Multi-frequency harmonic vibrations were generated by four small plastic driver pads driven by compressed-air pulses with 0.6-bar amplitude (size 8.0 × 4.0 × 1.0 cm), which were placed on the anterior (two pads) and posterior (two pads) surface projection of the pancreas. Parallel imaging with an acceleration factor of two was used with eight time steps over a vibration period. During free breathing, 3D wave fields with four vibration frequencies of 30, 40, 50, and 60 Hz were acquired continuously. Multi-frequency wave field data were obtained using a single-shot, spin-echo, echo planar imaging sequence with flow-compensated, first-order motion-encoding gradients (MEGs) using frequencies of 37.20, 37.20, 37.48, and 44.88 Hz, and a MEG amplitude of 45 mT/m. The entire pancreas, covered by 35 contiguous axial sections, was scanned in 7 minutes and 22 seconds. Table 1 lists additional imaging parameters.

Tomoelastography image post-processing

We processed the multi-frequency wave field data using the processing pipeline available at https://bioqic-apps.com. The multi-frequency wave number-based processing algorithm generated full field-of-view, high-spatial-resolution maps of the shear wave speed (c) [12]. As c was directly proportional to the square root of the storage modulus (the real part of complex shear modulus), it was considered a substitute for tissue stiffness [13]. The Laplacian operators-based processing method generated the phase angle of the complex shear modulus (φ) images [14]. The range of φ is 0 to $\pi/2$, which described the continuous transition of tissue's behavior from pure solid to pure fluid [15]. Hence, the φ parameter was related to the tissue fluidity. We used c and φ in the text to report quantitative measures while the terms "stiffness" and "fluidity" were reserved for describing qualitative changes.

Image analysis

Two radiologists with 12-year (Reader 1) and 6-year (Reader 2) experience using pancreatic MR imaging analysed the images using ImageJ software (version 1.51). The image data sets of the healthy volunteers were anonymous and case numbers were arranged randomly. The readers were blinded to the volunteers' sex, age, and BMI. Each reader evaluated measurements of pancreatic stiffness and fluidity, pancreatic diameter, and pancreatic fat fraction independently (marked as Reader 1A and

Table 1. Sequence parameters of the pancreatic magnetic resonance imaging protocol

Sequence	T2-haste-cor-bh	T2-trigger-tse-fs-tra	Vibe-q-dixon-tra-bh (6 Echos)	Contmre-pancreas[a]
TR/TE (ms)	1,000/77	2,000/78	9.00/1.05–2.46–3.69–4.92–6.15–7.38	4,140/69
FA (°)	160	103	4	90
Section thickness (mm)	5	3	2	2
FOV (mm)	400	350	426	256
Acquisition time (s)	18	300–400	20	431
Acquisition matrix	168 × 256	288 × 384	111 × 160	128 × 128
Acceleration factor	3	3	4	2
Receiver bandwidth (Hz/Px)	1,221	766	1,080	1,086

[a]Magnetic resonance elastography frequencies: 30.30, 40.00, 50.00, and 59.88 Hz.
TR, repetition time; TE, echo time; FA, flip angle; FOV, field of view; cor, coronal; bh, breath-hold; tse, turbo spin-echo; fs, fat-saturated; tra, transverse; VIBE, volume-interpolated breath-hold.

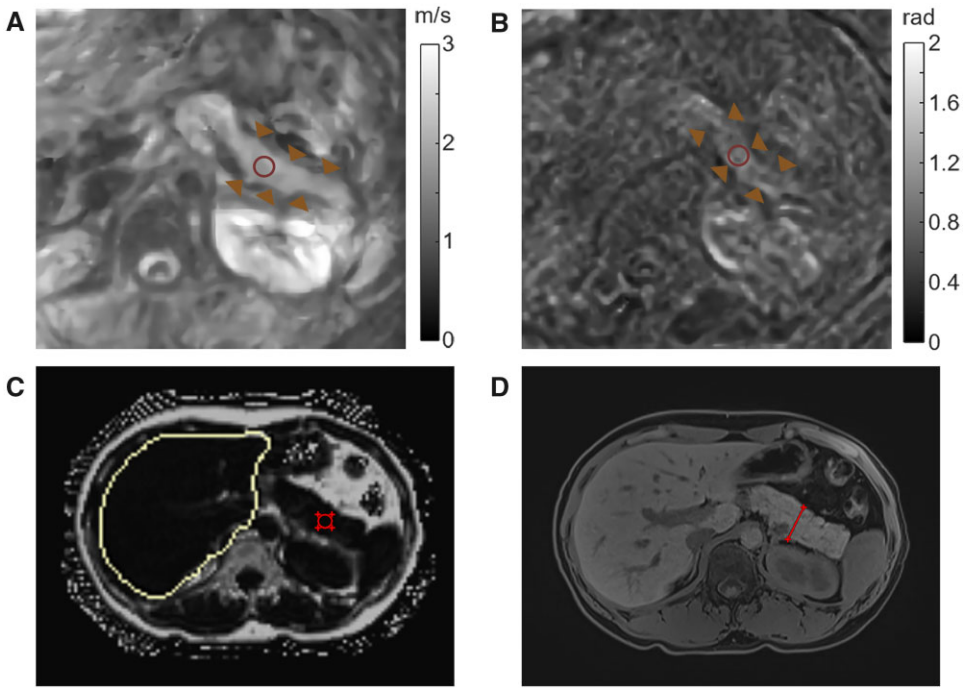

Figure 1. Examples of the regions of interest (ROIs) used to measure different variables. The ROIs are placed on the pancreas to measure pancreatic stiffness on the c map (A) and then copied to the φ map (B) to measure pancreatic fluidity. ROIs are placed on the pancreas to measure the pancreatic fat fraction (C) and pancreatic diameter (D) on the multi-echo Dixon image.

Reader 2). During the measurements of pancreatic stiffness and fluidity, the clearest and largest slices of the pancreas at the c map and φ map were selected and then adjusted to the appropriate brightness and contrast. Manually drawn regions of interest (ROIs) (~1.0 cm in diameter) were then placed on the segments of the head, body, and tail on the c map to measure stiffness. These ROIs on the c map were copied to the φ map to measure fluidity. Reader 1 repeated the measurements 2 weeks later (marked as Reader 1B). Reader 1 also measured the adjacent slices for pancreatic stiffness and fluidity (marked as Reader 1C). We measured the largest width of the pancreas to represent the pancreatic diameter. During the measurements of the pancreatic fat fraction, the ROIs were placed on the pancreatic head, body, and tail on multi-echo Dixon images and the mean value of three regional fat fractions was calculated (Figure 1). Reader 1 then measured the pancreatic stiffness and fluidity at the second examination (marked as Reader 1D).

Statistical analysis

Continuous data were averaged and are expressed as means ± standard deviation if normally distributed according to the Shapiro–Wilk test or as medians (interquartile range) if non-normally distributed. Categorical data are presented as numbers (percentages) and were compared using the chi-square test or Fisher's exact test. Inter-observer and intra-observer agreements were assessed using Bland–Altman analysis and intraclass correlation coefficients (ICCs). The inter-observer agreement was graded as follows: 0–0.20, slight; 0.21–0.40, fair; 0.41–0.60, moderate; 0.61–0.80, substantial; and 0.81–1.00, near perfect [16]. To compare the differences among pancreatic anatomical regions, the stiffness and fluidity of the pancreatic head, body, and tail were compared using an analysis of variance or Kruskal–Wallis test according to the variance homogeneity test. The variables were compared by sex, age, and BMI, and violin plots were drawn accordingly. A value of $P < 0.05$ was considered statistically significant.

Results

We enrolled 47 healthy volunteers, 32 of whom were women. For the entire cohort, the median age was 30 years (range, 23–59 years) and the mean BMI was 21.91 ± 2.89 kg/m^2.

The ICC values were 0.907–0.969 for pancreatic stiffness and 0.958–0.976 for pancreatic fluidity (all $P < 0.001$). The Bland–Altman analysis and ICCs demonstrated near perfect intra-observer agreements, slices, and short-term reproducibility. Figure 2 shows the detailed results.

The pancreatic head, body, and tail stiffnesses were 1.43 ± 0.12, 1.46 ± 0.15, and 1.46 ± 0.10 m/s, respectively. The pancreatic head, body, and tail fluidity values were 0.83 ± 0.08, 0.84 ± 0.10, and 0.82 ± 0.08 rad, respectively. Stiffness ($P = 0.477$) and fluidity ($P = 0.368$) did not differ among the pancreatic anatomical regions. The mean pancreatic stiffness was 1.45 ± 0.09 m/s and the mean pancreatic fluidity was 0.83 ± 0.06 rad. Figure 3 shows the frequencies of the mean pancreatic stiffness and fluidity, which did not differ by sex, age, or BMI (Tables 2–4 and Figure 4).

Discussion

Tomoelastography is a promising technique for determining pancreatic stiffness and fluidity. We found that tomoelastography-derived pancreatic stiffness and fluidity were almost perfectly reproducible in healthy volunteers. The pancreatic stiffness and fluidity did not statistically differ by age, sex, or BMI in our cohort.

Early studies used direct-inversion, single-frequency MRE to measure pancreatic stiffness in healthy volunteers [17, 18]. However, many factors are reported to affect pancreatic stiffness, indicating that more effective drivers and noise-robust image processing are needed to resolve the confounding factors when performing pancreatic MRE [19]. Tomoelastography is potentially less affected by noise than other MRE techniques

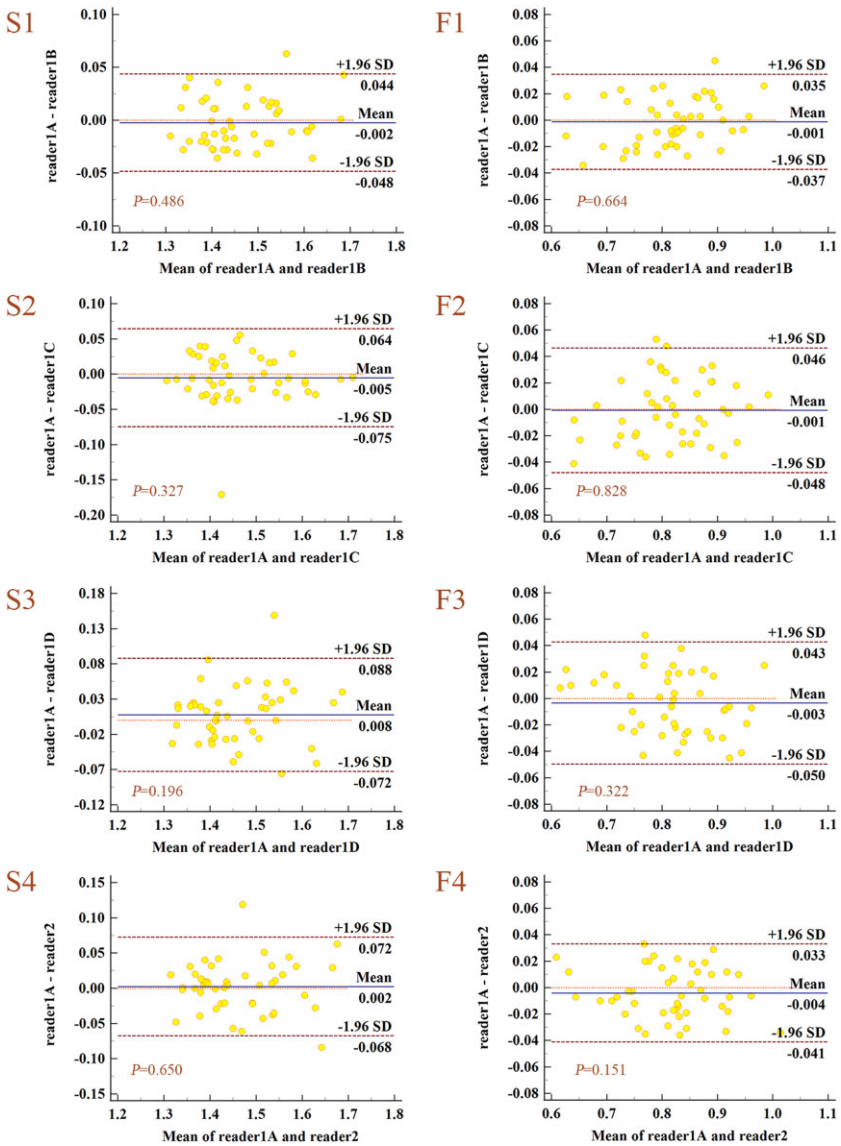

Figure 2. Bland–Altman analyses of reader agreement, slice selection, and short-term reproducibility. Reader 1A: Reader 1 measured the images from the first examination. Reader 1B: Reader 1 measured the images from the first examination, separated by a 2 week interval. Reader 1C: Reader 1 measured the adjacent slice of the images from the first examination. Reader 1D: Reader 1 measured the images from the second examination. Reader 2: Reader 2 measured the images from the first examination. S1–4: Bland–Altman analyses of reader agreements in pancreatic stiffness; F1–4: Bland–Altman analyses of reader agreements in pancreatic fluidity.

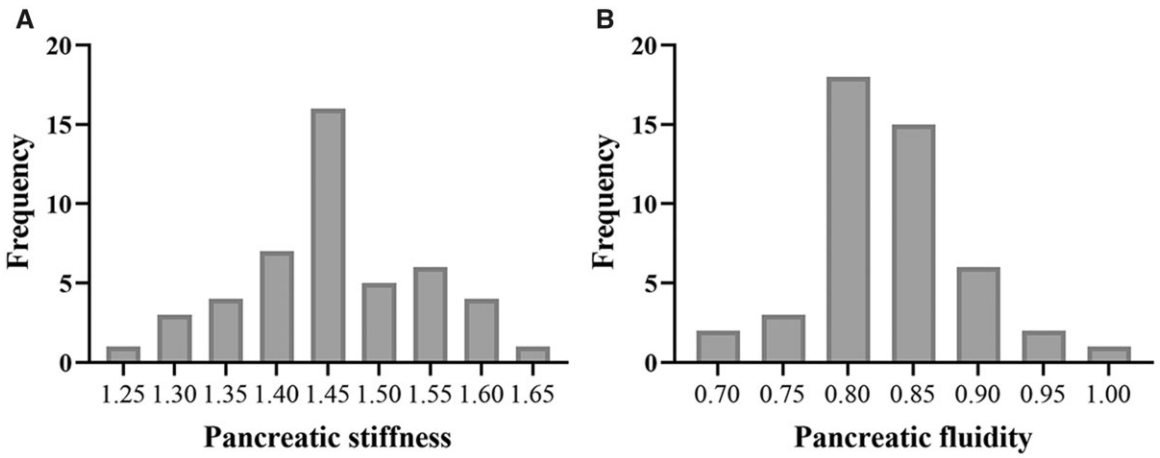

Figure 3. Frequencies of pancreatic stiffness (A) and fluidity (B)

Table 2. Comparison of variables by sex

Variable	Total ($n=47$)	Female ($n=32$)	Male ($n=15$)	P
Age (years)	30 (26, 49)	27.5 (25, 46)	45 (29, 50)	0.027*
BMI (kg/m^2)	21.91 ± 2.89	20.78 ± 1.92	24.32 ± 3.17	<0.001*
Stiffness (m/s)	1.45 ± 0.09	1.46 ± 0.08	1.44 ± 0.12	0.720
Fluidity (rad)	0.83 ± 0.06	0.83 ± 0.07	0.83 ± 0.05	0.885
Diameter (mm)	26.25 ± 4.22	26.43 ± 4.46	25.87 ± 3.79	0.660
Fat fraction	0.03 (0.02, 0.04)	0.02 (0.01, 0.03)	0.04 (0.03, 0.05)	<0.001*

BMI, body index mass.
*$P < 0.05$.

Table 3. Comparison of variables by age

Variable	Total ($n=47$)	Age <40 years ($n=30$)	Age ≥40 years ($n=17$)	P
Sex				0.484
Female	32 (68%)	22 (73%)	10 (59%)	
Male	15 (32%)	8 (27%)	7 (41%)	
BMI (kg/m^2)	21.91 ± 2.89	20.96 ± 2.6	23.58 ± 2.65	0.002*
Stiffness (m/s)	1.45 ± 0.09	1.46 ± 0.09	1.44 ± 0.09	0.479
Fluidity (rad)	0.83 ± 0.06	0.83 ± 0.06	0.83 ± 0.07	0.827
Diameter (mm)	26.25 ± 4.22	26.98 ± 4.23	24.96 ± 4.01	0.113
Fat fraction	0.03 (0.02, 0.04)	0.02 (0.01, 0.03)	0.04 (0.03, 0.05)	<0.001*

BMI, body index mass.
*$P < 0.05$.

Table 4. Comparison of variables by BMI

Variable	Total ($n=47$)	BMI <24 kg/m^2 ($n=37$)	BMI ≥24 kg/m^2 ($n=10$)	P
Sex				<0.001*
Female	32 (68%)	31 (84%)	1 (10%)	
Male	15 (32%)	6 (16%)	9 (90%)	
Age (years)	30 (26, 49)	28 (26, 46)	42 (30.25, 49.75)	0.062
Stiffness (m/s)	1.45 ± 0.09	1.46 ± 0.09	1.43 ± 0.11	0.512
Fluidity (rad)	0.83 ± 0.06	0.83 ± 0.06	0.83 ± 0.06	0.929
Diameter (mm)	26.25 ± 4.22	26.27 ± 4.63	26.18 ± 2.34	0.931
Fat fraction	0.03 (0.02, 0.04)	0.03 (0.01, 0.03)	0.04 (0.03, 0.05)	0.012*

BMI, body index mass.
*$P < 0.05$.

because it uses multiple drivers and extracts shear wave speed through single-order derivative operators [6]. During standard direct inversion, this single-order, finite-difference operator propagates less noise than a second-order operator [12]. Additionally, the robustness of tomoelastography-derived pancreatic stiffness must be determined because the pancreas is an elongated organ deep in the abdomen. In this study, the inter-observer and intra-observer agreements for the pancreatic stiffness and fluidity measurements were nearly perfect, indicating that tomoelastography-derived pancreatic stiffness was reproducible, which was similar to the findings of other studies [5, 6]. Notably, no extensive training is needed to measure pancreatic stiffness and fluidity; therefore, the quantitative tomoelastography-derived pancreatic stiffness and fluidity data should be applicable and reliable for radiologists. Tomoelastography technology should be standardized to better screen pancreatic diseases and promote this technology in clinical work. Consistently with the current study, previous studies have shown good consistency between readers [5, 6]. Our study also indicated near perfect repeatability among slices and short-term intervals for the first time.

In two studies that used the same tomoelastography protocol, the mean pancreatic stiffness values were 1.25 ± 0.09 m/s (mean age, 44 years) [6] and 1.32 ± 0.05 m/s (median age, 52 years) [5], which were slightly lower than the measurements found in our study (1.45 ± 0.09 m/s; median age, 30 years). This may be due to possible age, sex, and BMI distribution biases within cohorts. Recent studies have reached inconsistent conclusions regarding the effect of pancreatic stiffness. Some studies indicated that age, sex, and BMI affected pancreatic stiffness [19–21], whereas other studies failed to establish associations between these parameters [6, 22], which is consistent with our results. Moreover, one study has found that both fat and fibrosis increased with age [23], whereas other studies showed no association [24] or negative association between these factors [25]. These contradictory results might be attributable to age, sex, and BMI distribution biases within cohorts. The pancreas can undergo age-related changes, such as fibrosis, fat replacement, and lobular central atrophy [26, 27]. Theoretically, an aging pancreas may stiffen owing to ongoing fibrosis and the influx of

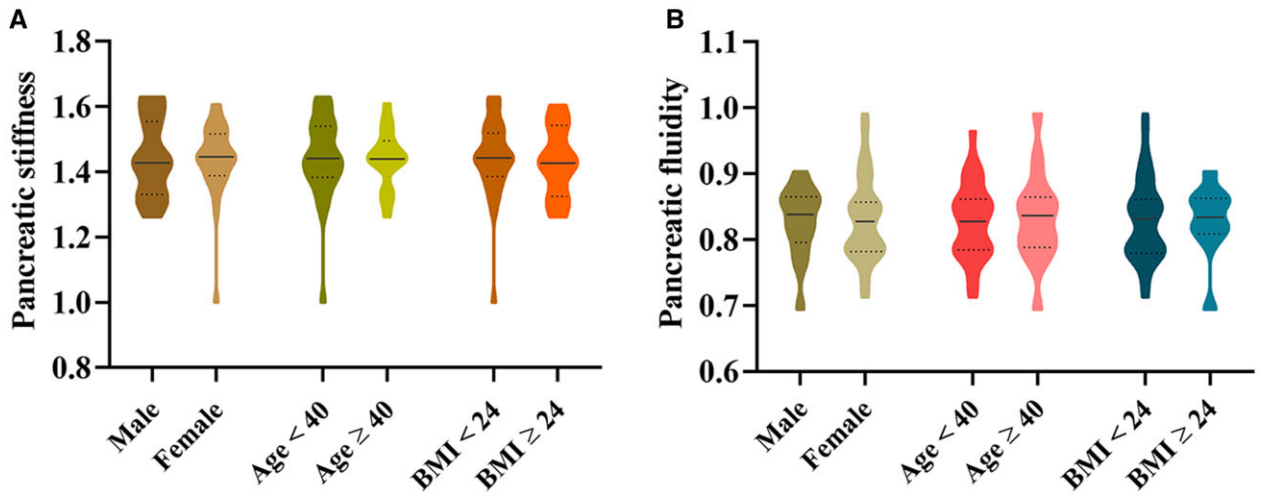

Figure 4. Violin plots of the distributions of pancreatic stiffness (A) and fluidity (B) based on sex, age, and body mass index (BMI)

lymphoplasmic cells [28]. However, parenchymal atrophy or fatty deposition may cause the pancreas to soften [19]. The detailed mechanisms of fibrogenesis and fatty deposition interactions and their effects on pancreatic stiffness require further study. Another study found no regional variation in pancreatic stiffness values across the pancreatic sub-regions in healthy individuals [6], which was consistent with our results using the same tomoelastography protocol.

It is necessary to understand the role of pancreatic fluidity; however, at present, few studies have analysed the fluidity of tissues and organs in normal or diseased states. Fluidity is reported to be unassociated with water content in tissues, and increases even after the material dries [29]. Notably, Shahryari *et al.* [15] showed that fluidity φ is related to both the amount of water in biological tissues and the inherent mechanical friction induced by extracellular matrix components or cell adhesion. To our knowledge, only one study has discussed pancreatic fluidity [5]. Zhu *et al.* [5] observed that fluidity increased as the stiffness increased in patients with pancreatic cancer and autoimmune pancreatitis compared with those of healthy individuals. During pancreatic cancer development and progression, some events may help increase fluidity, such as activation of stellate cells and accumulation of hydrophobin in the extracellular matrix of the tumor, depletion of glycosaminoglycans, and transition of the collagen content from an organized chain pattern to a more randomly aligned pattern [5]. Fluidity of the distal pancreatic parenchyma in pancreatic ductal adenocarcinoma was reported to be unaffected by obstruction [5], indicating that the microenvironment of the pancreatic parenchyma remained stable, and that the solid and fluid biomechanical properties of the pancreatic parenchyma were almost unchanged by obstructive changes. Zhu *et al.* [5] found that the mean pancreatic fluidity was 0.81 ± 0.04 rad, which was similar to our results (0.83 ± 0.06 rad). These results should be verified using more participants with wider age and BMI distributions. More studies are needed to better understand the characteristics of pancreatic fluidity.

Fibrosis and inflammatory cell infiltration due to CP and pancreatic ductal adenocarcinoma lead to histological changes in normal pancreatic structures. These mechanical property changes provide an impetus for exploring tomoelastography as a potential tool for detecting the stiffness and fluidity of the pancreas of patients with pancreatic diseases. In our study, tomoelastography-derived pancreatic stiffness and fluidity in healthy volunteers were almost perfectly reproducible between readers, slices, and examinations at short intervals. These normal range values of pancreatic stiffness and fluidity can be used as a reference for pancreatic diseases in young and middle-aged, non-obese patients.

Although these results are encouraging, this study had several limitations. First, the sample size was relatively small, and the age and BMI distributions were not broad enough. Future studies should enroll patients with a higher BMI and older patients with pancreatic atrophy and fatty infiltration. Second, this study enrolled only healthy volunteers; therefore, further research is needed to determine a reference range for specific diseases. Finally, we did not confirm the absence of pancreatic diseases in our volunteers through serological testing or other imaging examinations. Although the participants were thoroughly screened by reviewing their medical history and existing medical records, the possibility of unknown or unrecognized pancreatic disease remains.

Conclusions

In summary, tomoelastography is a robust, multi-frequency MRE technique that can provide reproducible pancreatic stiffness and fluidity measurements. These data will enable future studies of tomoelastography as a potential clinical tool.

Authors' Contributions

Y.L., S.Y.S., Z.P., and L.W. conceived and designed the project; Y.W., Z.L., X.H., J.Y., L.H., and S.T.F. collected the data; Y.L., S.Y.S., L.W., and Z.P. analysed and interpreted the data; Y.L., S.Y.S., L.W., and Z.P. drafted the manuscript. All authors read and approved the final manuscript.

Funding

This work was supported by the National Natural Science foundation of China [grant number 81801761 to Y.L.].

Acknowledgements

The authors sincerely acknowledge Ms Jing Guo from Department of Radiology of Charité—Universitätsmedizin Berlin, Germany for the MR technical support.

Conflict of Interest

None declared.

References

1. Siegel RL, Miller KD, Jemal A. Cancer statistics, 2020. *CA A Cancer J Clin* 2020;**70**:7–30.
2. Mizrahi JD, Surana R, Valle JW *et al.* Pancreatic cancer. *Lancet* 2020;**395**:2008–20.
3. Conwell DL, Lee LS, Yadav D *et al.* American pancreatic association practice guidelines in chronic pancreatitis: evidence-based report on diagnostic guidelines. *Pancreas* 2014;**43**: 1143–62.
4. Janssen J, Schlorer E, Greiner L. EUS elastography of the pancreas: feasibility and pattern description of the normal pancreas, chronic pancreatitis, and focal pancreatic lesions. *Gastrointest Endosc* 2007;**65**:971–8.
5. Zhu L, Guo J, Jin ZY *et al.* Distinguishing pancreatic cancer and autoimmune pancreatitis with in vivo tomoelastography. *Eur Radiol* 2021;**31**:3366–74.
6. Garcia SMR, Zhu L, Gultekin E *et al.* Tomoelastography for measurement of tumor volume related to tissue stiffness in pancreatic ductal adenocarcinomas. *Invest Radiol* 2020;**55**: 769–74.
7. Apte MV, Park S, Phillips PA *et al.* Desmoplastic reaction in pancreatic cancer: role of pancreatic stellate cells. *Pancreas* 2004;**29**:179–87.
8. Sinha A, Singh VK, Cruise M *et al.* Abdominal CT predictors of fibrosis in patients with chronic pancreatitis undergoing surgery. *Eur Radiol* 2015;**25**:1339–46.
9. Shi Y, Gao F, Li Y *et al.* Differentiation of benign and malignant solid pancreatic masses using magnetic resonance elastography with spin-echo echo planar imaging and three-dimensional inversion reconstruction: a prospective study. *Eur Radiol* 2018;**28**:936–45.
10. Muthupillai R, Ehman RL. Magnetic resonance elastography. *Nat Med* 1996;**2**:601–3.
11. Hirsch S, Guo J, Reiter R *et al.* MR elastography of the liver and the spleen using a piezoelectric driver, single-shot wave-field acquisition, and multifrequency dual parameter reconstruction. *Magn Reson Med* 2014;**71**:267–77.
12. Tzschatzsch H, Guo J, Dittmann F *et al.* Tomoelastography by multifrequency wave number recovery from time-harmonic propagating shear waves. *Med Image Anal* 2016;**30**:1–10.
13. Hu J, Guo J, Pei Y *et al.* Rectal tumor stiffness quantified by in vivo tomoelastography and collagen content estimated by histopathology predict tumor aggressiveness. *Front Oncol* 2021;**11**:701336.
14. Streitberger KJ, Diederichs G, Guo J *et al.* In vivo multifrequency magnetic resonance elastography of the human intervertebral disk. *Magn Reson Med* 2015;**74**:1380–7.
15. Shahryari M, Tzschatzsch H, Guo J *et al.* Tomoelastography distinguishes noninvasively between benign and malignant liver lesions. *Cancer Res* 2019;**79**:5704–10.
16. Min JH, Lee MW, Park HS *et al.* Interobserver variability and diagnostic performance of gadoxetic acid-enhanced MRI for predicting microvascular invasion in hepatocellular carcinoma. *Radiology* 2020;**297**:573–81.
17. Shi Y, Glaser KJ, Venkatesh SK *et al.* Feasibility of using 3D MR elastography to determine pancreatic stiffness in healthy volunteers. *J Magn Reson Imaging* 2015;**41**:369–75.
18. Kolipaka A, Schroeder S, Mo X *et al.* Magnetic resonance elastography of the pancreas: measurement reproducibility and relationship with age. *Magn Reson Imaging* 2017;**42**:1–7.
19. Xu Y, Cai X, Shi Y *et al.* Normative pancreatic stiffness levels and related influences established by magnetic resonance elastography in volunteers. *J Magn Reson Imaging* 2020;**52**: 448–58.
20. Chantarojanasiri T, Hirooka Y, Kawashima H *et al.* Age-related changes in pancreatic elasticity: when should we be concerned about their effect on strain elastography? *Ultrasonics* 2016;**69**:90–6.
21. Stumpf S, Jaeger H, Graeter T *et al.*; The Elasto-Study Group Ulm. Influence of age, sex, body mass index, alcohol, and smoking on shear wave velocity (p-SWE) of the pancreas. *Abdom Radiol* 2016;**41**:1310–6.
22. Puttmann S, Koch J, Steinacker JP *et al.* Ultrasound point shear wave elastography of the pancreas: comparison of patients with type 1 diabetes and healthy volunteers: results from a pilot study. *BMC Med Imaging* 2018;**18**:52.
23. Catanzaro R, Cuffari B, Italia A *et al.* Exploring the metabolic syndrome: nonalcoholic fatty pancreas disease. *World J Gastroenterol* 2016;**22**:7660–75.
24. van Geenen EJM, Smits MM, Schreuder TCMA *et al.* Smoking is related to pancreatic fibrosis in humans. *Am J Gastroenterol* 2011;**106**:1161–6.
25. Mathur A, Pitt HA, Marine M *et al.* Fatty pancreas: a factor in postoperative pancreatic fistula. *Ann Surg* 2007;**246**:1058–64.
26. Tariq H, Nayudu S, Akella S *et al.* Non-alcoholic fatty pancreatic disease: a review of literature. *Gastroenterology Res* 2016;**9**: 87–91.
27. Matsuda Y. Age-related pathological changes in the pancreas. *Front Biosci (Elite Ed)* 2018;**10**:137–42.
28. Akkaya HE, Erden A, Kuru Oz D *et al.* Magnetic resonance elastography: basic principles, technique, and clinical applications in the liver. *Diagn Interv Radiol* 2018;**24**:328–35.
29. Streitberger KJ, Lilaj L, Schrank F *et al.* How tissue fluidity influences brain tumor progression. *Proc Natl Acad Sci USA* 2020;**117**:128–34.